

Electronic Supplementary Information (ESI) for

Gold nanoparticles on OMS-2 for heterogeneously catalyzed aerobic oxidative α,β -dehydrogenation of β -heteroatom-substituted ketones

Daichi Yoshii,^a Xiongjie Jin,^a Takafumi Yatabe,^a Jun-ya Hasegawa,^b Kazuya Yamaguchi*^a
and Noritaka Mizuno*^a

^a*Department of Applied Chemistry, School of Engineering, The University of Tokyo,
7-3-1 Hongo, Bunkyo-ku, Tokyo 113-8656, Japan.*

E-mail: kyama@appchem.t.u-tokyo.ac.jp, tmizuno@mail.ecc.u-tokyo.ac.jp; Fax: +81-3-5841-7220

^b*Institute for Catalysis, Hokkaido University, Kita 21 Nishi 10, Kita-ku, Sapporo 001-0021, Japan.*

Experimental details

Instruments and reagents

Gas chromatography (GC) analyses were performed on Shimadzu GC-2014 equipped with a flame ionization detector (FID) and an InertCap-5 capillary column. GC mass spectrometry (GC-MS) spectra were recorded on Shimadzu GCMS-QP2010 equipped with an InertCap-5 capillary column at an ionization voltage of 70 eV. High performance liquid chromatography (HPLC) analyses were performed on a Shimadzu Prominence system using a UV detector (Shimadzu SPD-20A, 254 nm) equipped with an Inertsil ODS-3 column using a mixed solvent of methanol/water as an eluent (9/1 v/v). Liquid-state NMR spectra were recorded on JEOL JNM-ECA-500. ¹H and ¹³C NMR spectra were measured at 500 and 125 MHz, respectively, using tetramethylsilane (TMS) as an internal reference ($\delta = 0$ ppm). ICP-AES analyses for Au and Mn species in the reaction solution were performed on Shimadzu ICPS-8100. The atomic absorption spectrometry (AAS) analyses for K species in the reaction solution were performed on HITACHI Z-2000. TEM observations were performed on JEOL JEM-2000EX II. BET surface areas were measured on micromeritics ASAP 2010 and calculated from the N₂ adsorption isotherm with BET equation. XRD patterns were recorded on a Rigaku SmartLab diffractometer (Cu_{K α} , $\lambda = 1.5405$ Å, 45 kV, 200 mA). The XPS measurements were carried out on JEOL JPS-9000 using Mg K α radiation ($h\nu = 1253.6$ eV, 8 kV, 10 mA). OMS-2 (BET surface area: 106 m² g⁻¹) was prepared according to the literature procedure.^{S1} Al₂O₃ (BET: 160 m² g⁻¹, Cat. No. KHS-24, Sumitomo Chemical), TiO₂ (BET: 316 m² g⁻¹, Cat. No. ST-01, Ishihara Sangyo Kaisya), and CeO₂ (BET: 111 m² g⁻¹, Cat. No. 544841-25G, Aldrich) were commercially available. Solvents and substrates (except for **1f**) were obtained from Kanto Chemical, TCI, Wako, or Aldrich (reagent grade), and

purified prior to being used, if necessary.^{S2} Substrate **1f** was synthesized according to the literature procedure.^{S3}

Preparation of Au/OMS-2

OMS-2 (2.0 g) was added to an aqueous solution of $\text{HAuCl}_4 \cdot 4\text{H}_2\text{O}$ (8.3 mM, 60 mL). After the mixture was vigorously stirred at room temperature for 15 min, the pH of the solution was quickly adjusted to 10 by addition of an aqueous solution of NaOH (1.0 M). The resulting mixture was further stirred for 24 h. The solid was filtered off, washed with deionized water (4 L), and dried in vacuo to afford the supported hydroxide catalyst precursor. Then, the hydroxide precursor was calcined at 300 °C for 2 h, giving Au/OMS-2 as a dark brown powder (Au content: 4.1 wt%, average Au size: 3.9 nm). Au/ Al_2O_3 (Au content: 4.1 wt%, average Au size: 4.9 nm), Au/ TiO_2 (Au content: 2.9 wt%, average Au size: 2.2 nm), and Au/ CeO_2 (Au content: 4.6 wt%, average Au size: 3.5 nm) were prepared according to the same procedure except that the calcination temperature was 400 °C in the case of other supported gold catalysts.

Catalytic reaction

The catalytic reaction was typically carried out according to the following procedure. Au/OMS-2 (3.6 mol%, 85 mg), **1** (0.5 mmol), H_2O (2 mL), and a Teflon-coated magnetic stir bar were successively placed in a Pyrex glass reactor (volume *ca.* 20 mL). The reaction mixture was vigorously stirred at 50–90 °C, in 1 atm of air or O_2 . After the reaction was completed, an internal standard (biphenyl) and a large amount of acetone were added to the reaction mixture, and the conversion of **1** and the product yield were determined by GC analysis. As for isolation of products, the internal standard was not added. After the reaction, the catalyst was removed by filtration, and then the filtrate was dried with Na_2SO_4 and concentrated by evaporation. The crude product was subjected to column chromatography on silica gel, giving the pure product. The products were identified by GC-MS and NMR (^1H and ^{13}C) analyses.

Reuse experiments

The retrieved catalyst was washed with ethanol and acetone, and calcined at 300 °C in air for 2 h before being used for the reuse experiment. The XRD analysis of the catalyst before being calcined revealed that OMS-2 support gradually changed to Mn_3O_4 as the reuse experiment was repeated (Fig. S3), and the XRD pattern of the catalyst before being calcined hardly changed after the calcination at 300 °C. Furthermore, we confirmed by the AAS analysis that *ca.* 50% of the tunnel K^+ species in the fresh Au/OMS-2 catalyst leached into the reaction solution during the oxidative dehydrogenation of **1a** under the standard reaction conditions. Therefore, the formation of Mn_3O_4 is likely caused by the reduction of manganese species and the elimination of the tunnel K^+ species in

the OMS-2 support. Thus, once the Mn_3O_4 (stable spinel) structure is formed during the reaction, the reconstruction of the OMS-2 (hollandite) structure is not possible by the simple calcination. Although the structure of OMS-2 gradually changed to Mn_3O_4 , the catalyst could be reused keeping its high performance (Fig. S2), indicating that Mn_3O_4 is also a good support for Au nanoparticles.

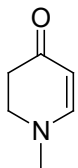
Plausible explanation for promotion effect of Br^-

As mentioned in the text, LiBr has the promotional effect on the Au/OMS-2-catalyzed oxidative dehydrogenation of **1d** to **2d** (Table S3, entry 1 vs. entry 2; Fig. S5, a, b). Other bromide salts, such as NaBr and KBr, also markedly promoted the dehydrogenation (Table S3, entries 3 and 4). In contrast, LiF, LiCl, and LiI did not promote the dehydrogenation (Table S3, entries 5–7). These results clearly indicate that Br^- can promote the Au/OMS-2-catalyzed oxidative dehydrogenation. When using Au/ Al_2O_3 , however, LiBr did not accelerate the dehydrogenation (Fig. S5, e, f). Moreover, in the case of using a physical mixture of Au/ Al_2O_3 and OMS-2, the dehydrogenation was also promoted by the addition of LiBr (Fig. S5, c, d). The redox potential of $\text{MnO}_2/\text{Mn}^{2+}$ is 1.23 V and higher than that of Br_2/Br^- (1.10 V).^{S4} Thus, it is possible that OMS-2 oxidizes Br^- into Br_2 , which likely oxidizes Au–H species to regenerate active Au species; hence, we consider the reaction in the presence of Br^- proceeds through multiple redox cycles (Scheme S2). Likely due to the relatively higher redox potentials of F_2/F^- (2.89 V) and Cl_2/Cl^- (1.39 V), the promotion of the dehydrogenation by F^- and Cl^- is less likely. Although the redox potential of I_2/I^- (0.62 V) is lower than that of $\text{MnO}_2/\text{Mn}^{2+}$, the dehydrogenation hardly proceeded in the presence of LiI (Table S3, entry 7). It is known that the interaction between I^- and Au nanoparticles is very strong,^{S5} hence, the reaction is probably inhibited in the presence of I^- .

Additional references

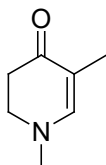
- S1 R. N. DeGuzman, Y.-F. Shen, E. J. Neth, S. L. Suib, C.-L. O'Young, S. Levine and J. M. Newsam, *Chem. Mater.*, 1994, **6**, 815.
- S2 W. L. F. Armarego and C. L. L. Chai, *Purification of Laboratory Chemicals*, Butterworth-Heinemann, Oxford, 5th edn, 2003.
- S3 T. Takeda and M. Terada, *J. Am. Chem. Soc.*, 2013, **135**, 15306.
- S4 S. G. Bratsch, *J. Phys. Chem. Ref. Data*, 1989, **18**, 1.
- S5 Z. Zhang, H. Li, F. Zhang, Y. Wu, Z. Guo, L. Zhou and J. Li, *Langmuir*, 2014, **30**, 2648.

Spectral data of β -heteroatom-substituted α,β -unsaturated ketones



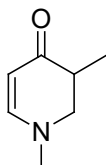
2a (CAS No. 35488-00-7)

2,3-Dihydro-1-methyl-4(1H)-pyridinone (2a): MS (EI, 70 eV): m/z (%): 111 (100) [M^+], 83 (23), 82 (44), 55 (43).



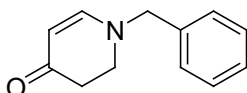
2b

2,3-Dihydro-1,5-dimethyl-4(1H)-pyridinone (2b): ^1H NMR (500 MHz, CDCl_3 , TMS): δ 1.68 (s, 3H), 2.48 (t, $J = 8.0$ Hz, 2H), 2.97 (s, 3H), 3.34 (t, $J = 8.0$ Hz, 2H), 6.88 (s, 1H). $^{13}\text{C}\{^1\text{H}\}$ NMR (125 MHz, CDCl_3 , TMS): δ 12.8, 35.7, 43.0, 49.5, 105.3, 153.8, 191.0.



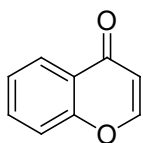
2b'

2,3-Dihydro-1,3-dimethyl-4(1H)-pyridinone (2b'): ^1H NMR (500 MHz, CDCl_3 , TMS): δ 1.14 (d, $J = 7.0$ Hz, 3H), 2.48 (m, 1H), 3.05 (s, 3H), 3.11 (m, 1H), 3.41 (m, 1H), 4.90 (d, $J = 7.0$ Hz, 1H), 6.95 (d, $J = 7.0$ Hz, 1H). $^{13}\text{C}\{^1\text{H}\}$ NMR (125 MHz, CDCl_3 , TMS): δ 13.8, 38.6, 43.1, 55.4, 97.0, 154.2, 194.6.



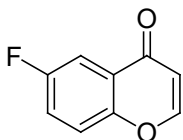
2c (CAS No. 35487-98-0)

2,3-Dihydro-1-(phenylmethyl)-4(1H)-pyridinone (2c): colorless oil. ^1H NMR (500 MHz, CDCl_3 , TMS): δ 2.46 (t, $J = 7.8$ Hz, 2H), 3.38 (t, $J = 7.8$ Hz, 2H), 4.37 (s, 2H), 5.00 (d, $J = 7.5$ Hz, 1H), 7.17 (d, $J = 7.5$ Hz, 1H), 7.26–7.41 (m, 5H). $^{13}\text{C}\{^1\text{H}\}$ NMR (125 MHz, CDCl_3 , TMS): δ 35.6, 46.7, 59.9, 98.5, 127.7, 128.4, 129.1, 135.8, 154.3, 191.6. MS (EI, 70 eV): m/z (%): 187 (36) [M^+], 96 (22), 92 (10), 91 (100), 65 (20).



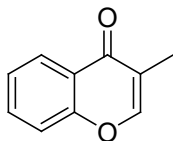
2d (CAS No. 491-38-3)

Chromone (2d): MS (EI, 70 eV): m/z (%): 147 (10), 146 (100) [M^+], 120 (22), 118 (65), 92 (51), 90 (18), 89 (14), 64 (22), 63 (32), 62 (10), 50 (17).



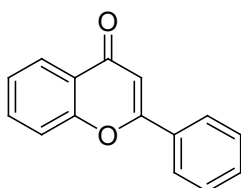
2e (CAS No. 105300-38-7)

6-Fluorochromone (2e): white solid. ^1H NMR (500 MHz, CDCl_3 , TMS): δ 6.34 (d, $J = 6.0$ Hz, 1H), 7.39–7.43 (m, 1H), 7.49 (dd, $J = 9.3$ and 4.3 Hz, 1H), 7.84 (dd, $J = 8.3$ and 3.3 Hz, 1H), 7.88 (d, $J = 6.0$ Hz, 1H). $^{13}\text{C}\{^1\text{H}\}$ NMR (125 MHz, CDCl_3 , TMS): δ 110.7 (d, $J = 23.9$ Hz), 112.4, 120.5 (d, $J = 7.2$ Hz), 122.2 (d, $J = 26.4$ Hz), 126.1 (d, $J = 7.2$ Hz), 152.8, 155.6, 159.6 (d, $J = 247$ Hz), 176.9. MS (EI, 70 eV): m/z (%): 165 (10), 164 (100) [M^+], 138 (23), 136 (45), 110 (31), 108 (12), 107 (10), 82 (19), 81 (11).



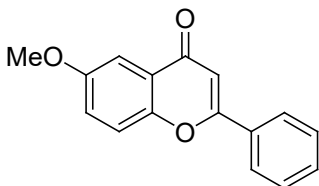
2f (CAS No. 85-90-5)

3-Methylchromone (2f): MS (EI, 70 eV): m/z (%): 161 (12), 160 (100) [M^+], 159 (11), 132 (20), 131 (59), 121 (11), 120 (26), 105 (11), 104 (17), 103 (16), 92 (39), 77 (15), 76 (10), 64 (16), 63 (17), 50 (11).



2g (CAS No. 525-82-6)

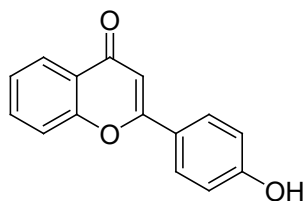
Flavone (2g): MS (EI, 70 eV): m/z (%): 223 (16), 222 (100) [M^+], 221 (32), 194 (52), 165 (15), 120 (76), 102 (20), 97 (19), 92 (76), 82 (16), 76 (17), 64 (29), 63 (29), 51 (13), 50 (14).



2h (CAS No. 26964-24-9)

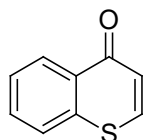
6-Methoxyflavone (2h): MS (EI, 70 eV): m/z (%): 253 (17), 252 (100) [M^+], 251 (76), 223 (17), 222

(25), 150 (64), 135 (20), 122 (17), 107 (45), 102 (25), 79 (55), 76 (14), 63 (16), 53 (16), 51 (25).



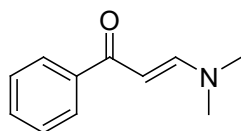
2i (CAS No. 4143-63-9)

4'-Hydroxyflavone (2i): pale yellow solid. ^1H NMR (500 MHz, DMSO- d_6 , TMS): δ 6.89 (s, 1H), 6.96 (d, $J = 9.0$ Hz, 2H), 7.48–7.51 (m, 1H), 7.75–7.77 (m, 1H), 7.80–7.84 (m, 1H), 7.98 (d, $J = 9.0$ Hz, 2H), 8.04–8.05 (m, 1H), 10.35 (brs, 1H). $^{13}\text{C}\{^1\text{H}\}$ NMR (125 MHz, DMSO- d_6 , TMS): δ 104.8, 116.0, 118.4, 121.6, 123.3, 124.8, 125.4, 128.4, 134.1, 155.6, 161.0, 163.1, 176.9. MS (EI, 70 eV): m/z (%): 239 (16), 238 (100) [M^+], 237 (34), 210 (23), 121 (57), 120 (12), 118 (32), 105 (13), 92 (27), 89 (16), 64 (17), 63 (20).



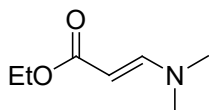
2j (CAS No. 491-39-4)

1-Thiochromone (2j): pale orange solid. ^1H NMR (500 MHz, CDCl_3 , TMS): δ 7.01 (d, $J = 10.0$ Hz, 1H), 7.53–7.56 (m, 1H), 7.60–7.61 (m, 2H), 7.83 (d, $J = 10.0$ Hz, 1H), 8.53–8.55 (m, 1H). $^{13}\text{C}\{^1\text{H}\}$ NMR (125 MHz, CDCl_3 , TMS): δ 125.95, 126.78, 127.92, 128.73, 131.52, 132.38, 137.61, 137.98, 179.79. MS (EI, 70 eV): m/z (%): 163 (10), 162 (100) [M^+], 136 (54), 135 (10), 134 (99), 108 (39), 89 (11), 82 (13), 74 (10), 69 (27), 67 (12), 63 (17), 58 (17), 50 (17).



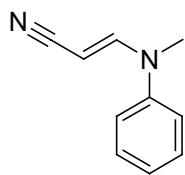
2k (CAS No. 1201-93-0)

3-(Dimethylamino)-1-phenyl-2-propen-1-one (2k): MS (EI, 70 eV): m/z (%): 175 (27) [M^+], 159 (10), 158 (82), 105 (25), 98 (100), 91 (18), 77 (59), 70 (45), 55 (48), 51 (37), 50 (12).



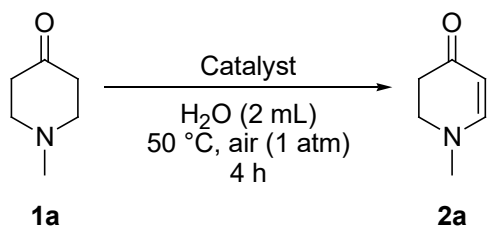
2l (CAS No. 924-99-2)

Ethyl 3-(dimethylamino)acrylate (2l): MS (EI, 70 eV): m/z (%): 143 (33) [M^+], 114 (19), 98 (100), 71 (30), 70 (22), 55 (20).



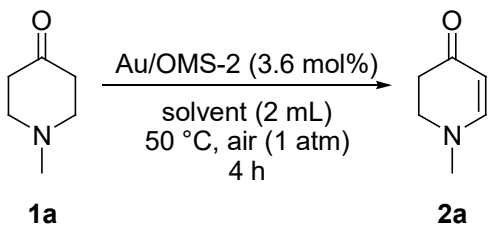
2m (CAS No. 76946-79-7)

3-(Methylphenylamino)-2-propenenitrile (2m): MS (EI, 70 eV): m/z (%): 159 (12), 158 (100) [M^+], 157 (41), 142 (27), 130 (15), 117 (45), 116 (20), 104 (12), 91 (22), 90 (11), 89 (13), 77 (51), 65 (12), 52 (12), 51 (37), 50 (10).

Table S1 Oxidative dehydrogenation of 1-methyl-4-piperidone (**1a**) using various catalysts^a

Entry	Catalyst	Conv. (%)	Yield (%)
1	Au/OMS-2	82 (94 ^b)	78 (90 ^b)
2	Pd/OMS-2	30	24
3	Ag/OMS-2	1	nd
4	Cu/OMS-2	7	nd
5	Ru/OMS-2	5	nd
6	Au/Al ₂ O ₃	71	66
7	Au/CeO ₂	59	55
8	Au/TiO ₂	54	54
9 ^c	Au/Al ₂ O ₃ + OMS-2	70	64
10 ^d	OMS-2	14	nd
11	None	<1	nd

^a Reaction conditions: **1a** (0.5 mmol), catalyst (metal: 3.6 mol%), H₂O (2 mL), 50 °C, air (1 atm), 4 h. Conversions and yields were determined by GC analysis. ^b 8 h. ^c A physical mixture of Au/Al₂O₃ (Au: 3.6 mol%) and OMS-2 (80 mg). ^d OMS-2 (80 mg).

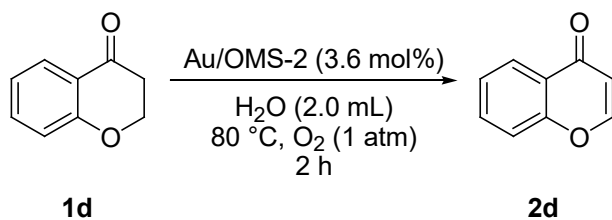
Table S2 Oxidative dehydrogenation of 1-methyl-4-piperidone (**1a**) in various solvents^a

Reaction scheme showing the oxidative dehydrogenation of 1-methyl-4-piperidone (**1a**) to 1-methyl-4,5-dihydropyridin-2(1H)-one (**2a**) using Au/OMS-2 (3.6 mol%) in a solvent (2 mL) at 50 °C, air (1 atm), for 4 h.

Entry	Solvent	Conv. (%)	Yield (%)
1	H ₂ O	82 (94 ^b)	78 (90 ^b)
2	Ethanol	60 (79 ^c)	60 (76 ^c)
3	<i>N,N</i> -Dimethylformamide	52	49
4	<i>N,N</i> -Dimethylacetamide	55	48
5	Acetonitrile	30	24
6	Toluene	21	16
7	1,4-Dioxane	17	13
8	Tetrahydrofuran	9	9

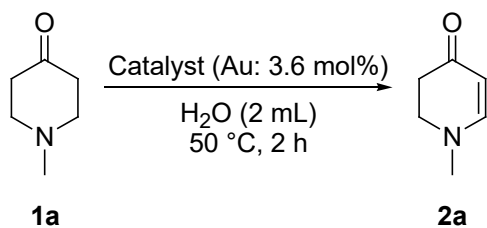
^a Reaction conditions: **1a** (0.5 mmol), Au/OMS-2 (Au: 3.6 mol%), solvent (2 mL), 50 °C, air (1 atm), 4 h. Conversions and yields were determined by GC analysis.
^b 8 h. ^c 12 h.

Table S3 Effect of additives on the oxidative dehydrogenation of 4-chromanone (**1d**)^a



Entry	Additive	Conv. (%)	Yield (%)
1	None	21	18
2	LiBr	41	38
3	NaBr	39	34
4	KBr	36	30
5	LiF	21	17
6	LiCl	19	16
7	LiI	3	1

^a Reaction conditions: **1d** (0.5 mmol), Au/OMS-2 (Au: 3.6 mol%), additive (1 mol%) H₂O (2.0 mL), 80 °C, O₂ (1 atm), 2 h. Yields were determined by GC analysis.

Table S4 Effect of TEMPO on the oxidative dehydrogenation of 1-methyl-4-piperidone (**1a**)^a

Entry	Catalyst	Atmosphere	Additive	Conv. (%)	Yield (%)
1			none	31	31
2	Au/Al ₂ O ₃	air (1 atm)	TEMPO (1 eq.)	41	40
3		Ar (1 atm)	none	<1	<1
4 ^b			TEMPO (1 eq.)	33	33
5			none	48	44
6	Au/OMS-2	air (1 atm)	TEMPO (1 eq.)	47	44
7 ^c		Ar (1 atm)	none	98	91
8	none	air (1 atm)	TEMPO (1 eq.)	<1	nd

^a Reaction conditions: **1a** (0.5 mmol), catalyst (Au: 3.6 mol%), H₂O (2 mL), 50 °C, 2 h. Conversions and yields were determined by GC analysis.

^b TEMPOH was formed in 60% (based on TEMPO). ^c 4 h.

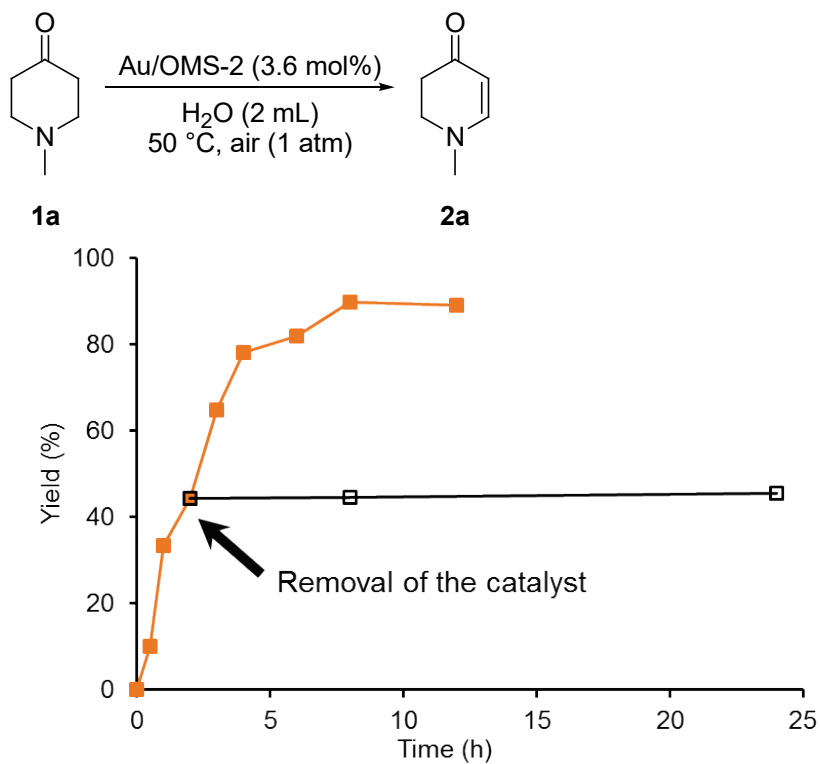


Fig. S1 Effect of removal of the Au/OMS-2 catalyst on the oxidative dehydrogenation of 1-methyl-4-piperidone (**1a**). The reaction conditions were the same as those described in Table S1. GC yields are shown here.

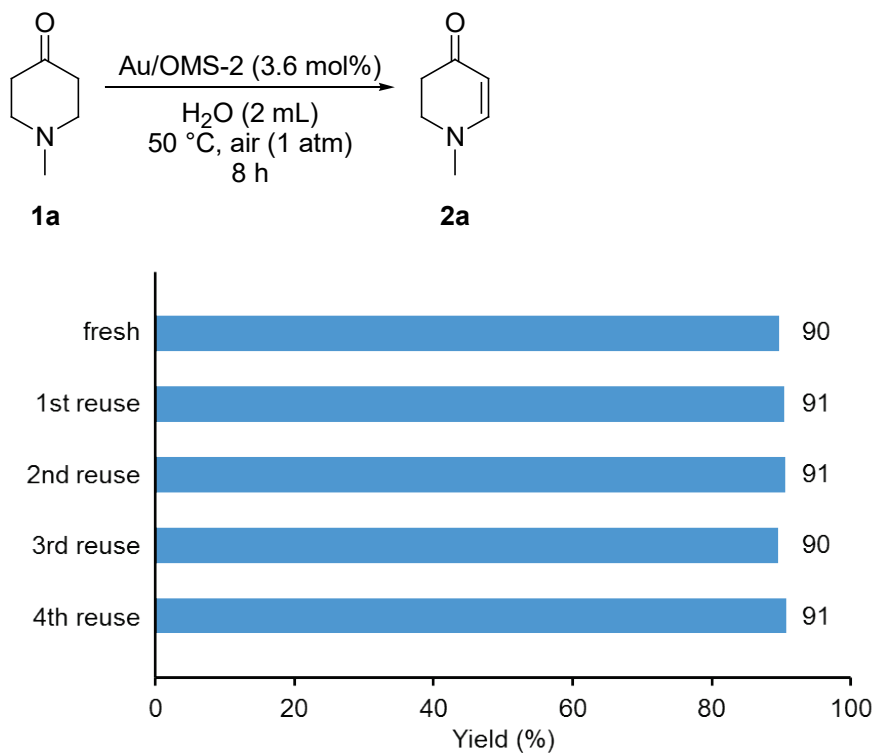


Fig. S2 Reuse experiments for the oxidative dehydrogenation of 1-methyl-4-piperidone (**1a**). Reaction conditions: **1a** (0.5 mmol) Au/OMS-2 (Au: 3.6 mol%), H₂O (2 mL), 50 °C, air (1 atm), 8 h. GC yields are shown here.

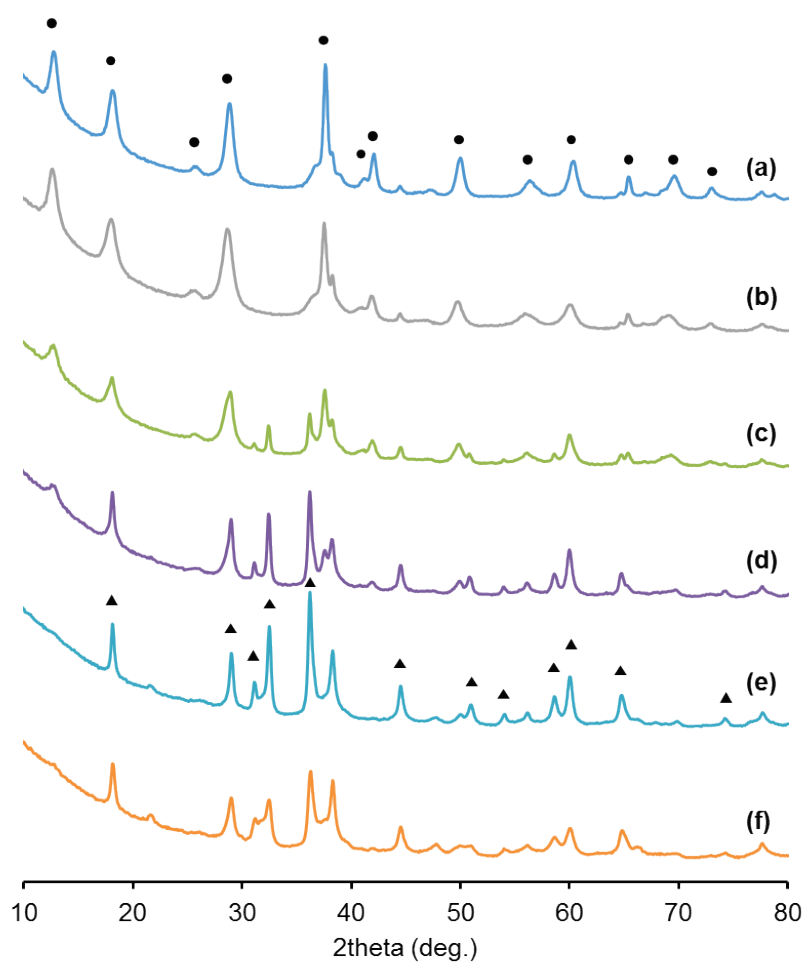


Fig. S3 XRD patterns of (a) the fresh Au/OMS-2, (b) Au/OMS-2 after the 1st use for the transformation of 1-methyl-4-piperidone (**1a**) under the conditions described in Fig. S2, (c) Au/OMS-2 after the 1st reuse experiment, (d) Au/OMS-2 after the 2nd reuse experiment, (e) Au/OMS-2 after the 3rd reuse experiment, and (f) Au/OMS-2 after the 4th reuse experiment. The closed circles (●) and triangles (▲) indicate the signals due to OMS-2 and Mn₃O₄, respectively.

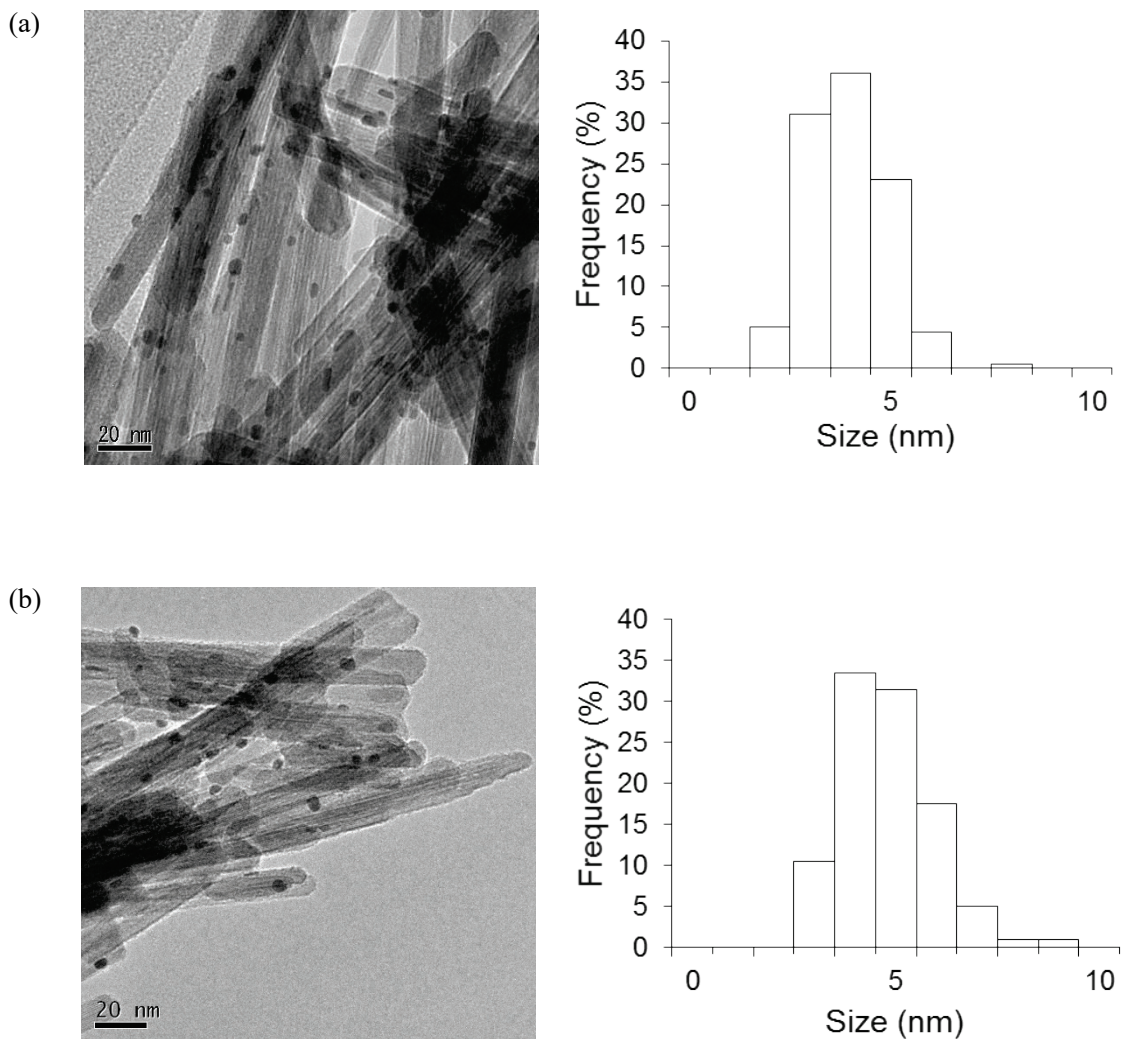


Fig. S4 TEM images and Au particles size distributions of (a) the fresh Au/OMS-2 (average: 3.9 nm, σ : 1.0 nm) and (b) Au/OMS-2 after the 1st use for the reaction of 1-methyl-4-piperidone (**1a**) under the conditions described in Fig. S2 (average 4.8 nm, σ : 1.1 nm). The size distributions were determined using 200 particles.

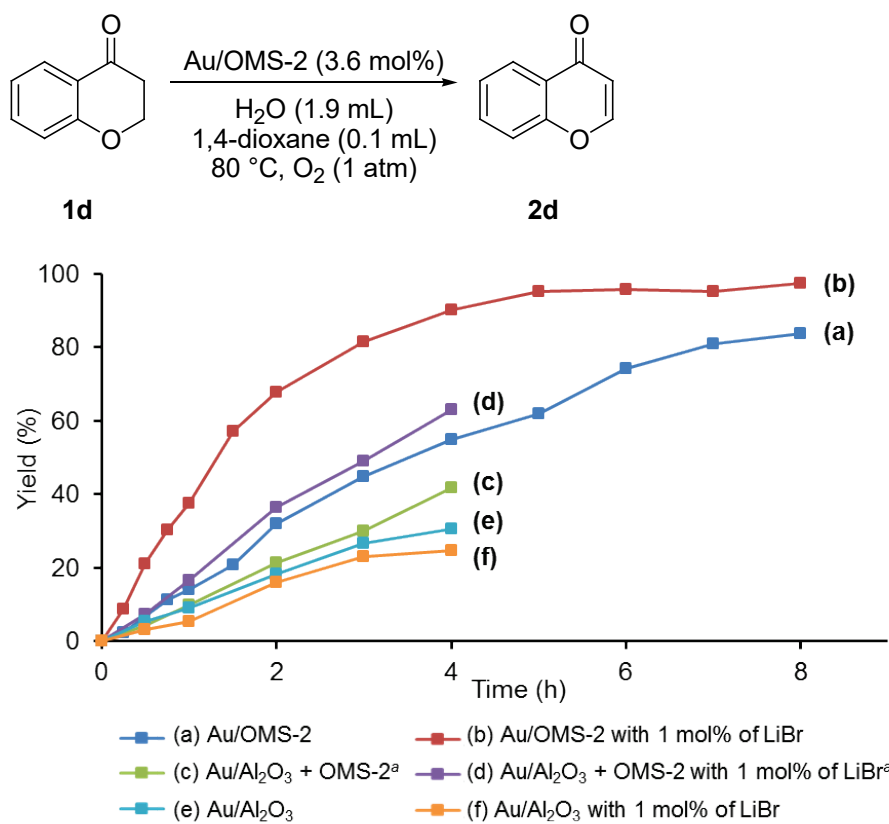


Fig. S5 Effect of LiBr on the oxidative dehydrogenation of 4-chromanone (**1d**). Reaction conditions: **1d** (0.5 mmol), Au/Support (Au: 3.6 mol%), H₂O (1.9 mL), 1,4-dioxane (0.1 mL), 80 °C, O₂ (1 atm). Yields were determined by GC analysis. ^a A physical mixture of Au/Al₂O₃ (Au: 3.6 mol%) and OMS-2 (80 mg).

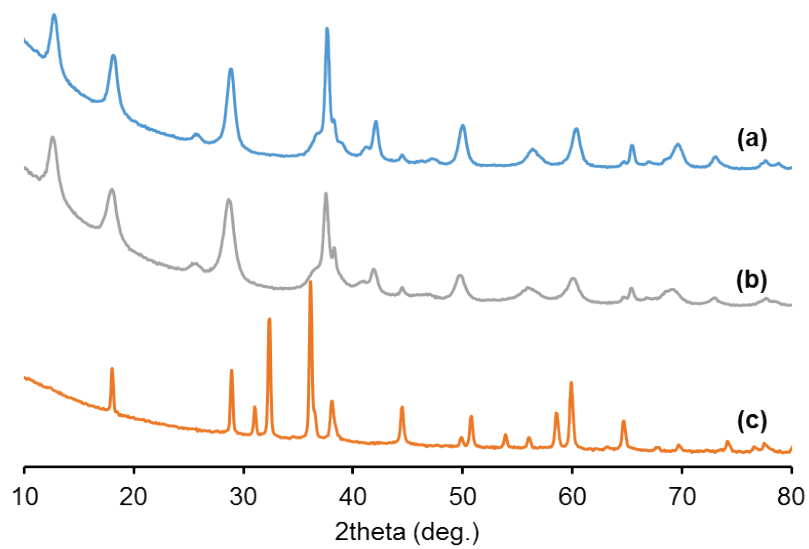


Fig. S6 XRD patterns of (a) the fresh Au/OMS-2, (b) Au/OMS-2 after the use for the transformation of 1-methyl-4-piperidone (**1a**) under the conditions described in Fig. S2 (under air) and (c) Au/OMS-2 after the use for the transformation of **1a** under the conditions described in Table S4, entry 7 (under Ar).

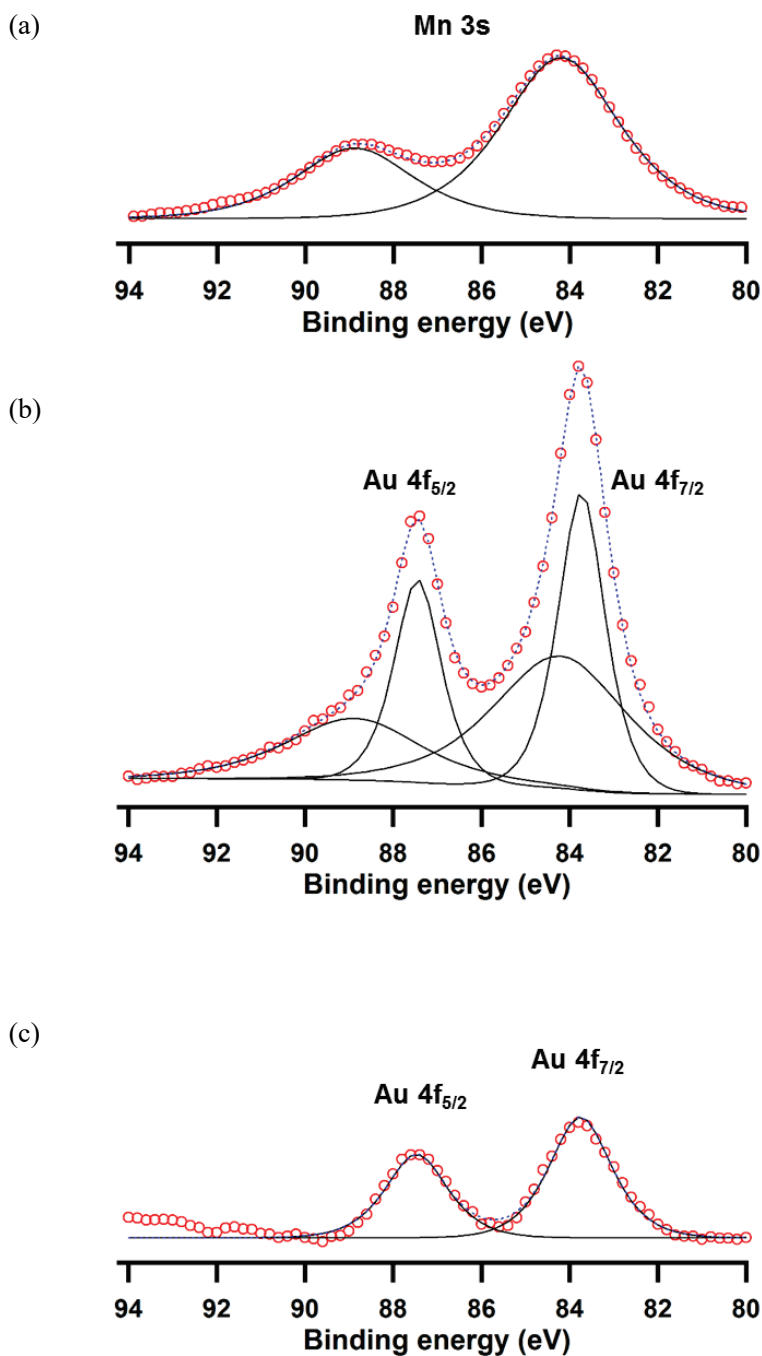
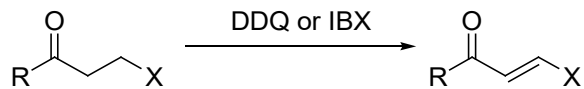


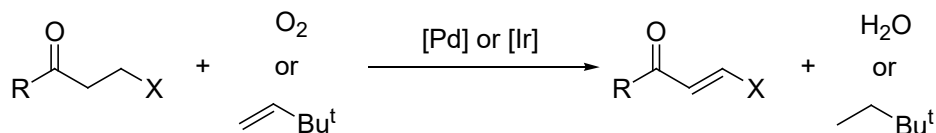
Fig. S7 XPS spectra of (a) OMS-2, (b) Au/OMS-2 and (c) Au/Al₂O₃ around Au 4f components. The red circles indicate the data points. The solid and broken lines indicate the deconvoluted signals and the sum of the deconvoluted signals, respectively. The Au 4f_{7/2} peaks of Au/OMS-2 and Au/Al₂O₃ were observed at 83.7 eV and 83.8 eV, respectively. Therefore, the average valence states of Au in Au/OMS-2 and Au/Al₂O₃ are the same and both zero, and the valence states are hardly affected by these supports.

(a) Previous work

■ Dehydrogenation by stoichiometric reagents

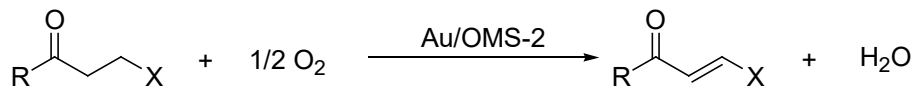


■ Dehydrogenation by homogeneous Pd or Ir catalysts

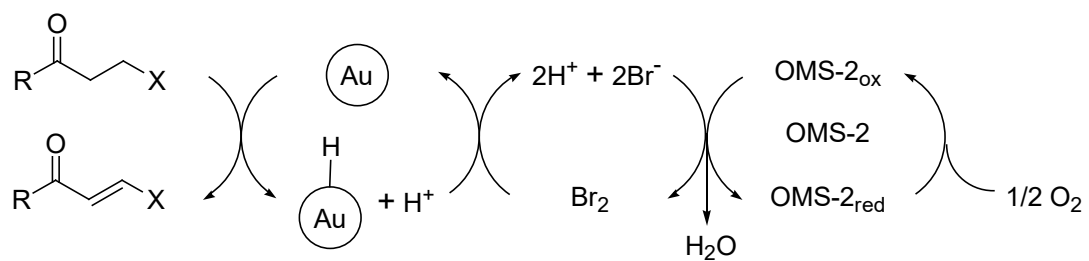


(b) This work

■ Dehydrogenation by heterogeneous Au catalyst



Scheme S1 α,β -Dehydrogenation of saturated ketones. X = NR'R', OR', SR'; R, R' = alkyl, aryl.



Scheme S2 Possible mechanism for the Au/OMS-2-catalyzed oxidative dehydrogenation promoted by Br^- .